

Received December 26, 2018, accepted January 15, 2019, date of publication January 23, 2019, date of current version February 20, 2019.

Digital Object Identifier 10.1109/ACCESS.2019.2894341

# Real-Time Observation of Range-Averaged Temperature by High-Frequency Underwater Acoustic Thermometry

XIAOJIAN YU<sup>1</sup>, XIAOBING ZHUANG<sup>2</sup>, YANLONG LI<sup>3</sup>, AND YU ZHANG<sup>1,2</sup>

<sup>1</sup>School of Biological Science and Biotechnology, Minnan Normal University, Zhangzhou 363000, China

<sup>2</sup>Key Laboratory of Underwater Acoustic Communication and Marine Information Technology of the Ministry of Education, Xiamen University, Xiamen 361000, China

<sup>3</sup>Department of Architecture, Xiamen University, Xiamen 361005, China

Corresponding author: Yu Zhang (yuzhang@xmu.edu.cn)

This work was supported in part by the Xiamen Institute of Science and Technology ([2017]C12) in part by the National Key Research and Development Program of China under Grant 2016YFC0502901 and Grant 2018YFC1407504, in part by the National Science Foundation of China under Grant 41676023, Grant 41276040, Grant 41422604, and Grant 11174240, and in part by the Natural Science Foundation of Fujian Province of China under Grant 2012J06010.

**ABSTRACT** Temperature has a great impact on the underwater environment in oceans. The real-time monitoring of it is of both scientific and practical importance. In this paper, we proposed a new scheme of high-frequency acoustic thermometry to measure the real-time ranged-averaged underwater temperature. The cross-correlation analysis with high-resolution Global Positioning System synchronization was used to derive the propagation time of underwater acoustic signals. Reciprocal underwater acoustic transmissions between two acoustic stations extracted the range-averaged temperature. Furthermore, a field experiment of high-frequency acoustic transmission was performed in the Jiulong River estuary. The ranged-average temperature extracted by the underwater acoustic sensor was compared with *in situ* temperature with a relative standard deviation of about 6%. The range-averaged temperature was correlated with *in situ* temperature ( $R^2 = 0.93$ ) during 48-hour real-time measurement experiments. The results suggest the potential applications of proposed high-frequency acoustic thermometry in real-time monitoring of the averaged temperature in coastal oceans.

**INDEX TERMS** Underwater high-frequency acoustics, range-averaged temperature, real-time monitoring.

## I. INTRODUCTION

Water temperature plays an important role in the biological, chemical, and physical properties of underwater ecosystems [1], [2]. Real-time water temperature monitoring is of great scientific and practical significance. Thermometers and conductivity-temperature-depth sensors, which are most commonly used, offer in-situ measurement of water temperature. However, they are incapable of obtaining real-time ranged-average temperature, particularly during flood periods. Therefore, a long-term scheme is necessary for ranged-average temperature monitoring in shallow water areas.

Underwater acoustic sensing has been widely used in a variety of ocean applications, such as exploring

ocean resources or monitoring ocean environments [3]–[6]. Recently, low frequency acoustic techniques have been developed to measure averaged seawater temperature over a long distance [2]–[8]. Acoustic thermometry of ocean climate project was conducted to monitor global warming [2]. The arctic climate observation using underwater sound project measured the temperature variation of arctic ocean water [3]. However, for coastal oceans or estuaries with much smaller space scales, low frequency acoustic thermometry is difficult to be applied due to its low spatial resolution [9]–[12]. Due to the superimposed effects of human activities and climate change, there is an urgent demand for developing high-frequency acoustic techniques to monitor highly variant underwater temperatures.

In this paper, we propose high frequency acoustic thermometry (HFAT) as a new real-time scheme to measure range-averaged underwater temperature. High resolution

The associate editor coordinating the review of this manuscript and approving it for publication was Guangjie Han.

Global Positioning System (GPS) time synchronization and cross-correlation analysis are employed to derive the propagation time of underwater acoustic signals. Using a field experiment in the Jiulong River Estuary, we compare the resulting temperatures by HFAT with the in-situ temperature measured by digital thermometer.

The rest of this paper is organized as follows: Descriptions about this system are given in Section II. The HFAT underwater experiment is described to assess the accuracy of the system, the comparison with in-situ thermometer is presented in Section III, and concluding remarks are given in Section IV.

## II. MATERIALS AND METHODS

Acoustic reciprocal transmission principle can be used to extract range-averaged temperature [13]–[15]. As shown in Fig. 1(a), the system consists of a pair of acoustic stations (A and B) placed on both sides of shallow waters. Acoustic station was achieved by the 20GP container, with an external size of  $5.9 \times 2.35 \times 2.39$  m. The wall was double steel plates with a thickness of 60 mm. The roof was covered with 50 mm thick rock wool. We designed the stations in Fig. 1(b) by integrating facilities, such as solar panels, power supply,

power circuit, water pump, drain pipe, work bench, and power control. Real-time monitoring instrument with Wifi connections was set in the container. Such an infrastructure provides an efficient platform for hydrological monitoring in estuarine area.

For Stations A and B, underwater acoustic transducers and hydrophones transmit and receive the signals, respectively. The reciprocal travel times of acoustic waves between the two stations can be written as [9], [11]–[13], [15]–[17]:

$$t^+ = \int \frac{ds}{C + \delta c + |u \cdot \cos \theta|} \quad (1)$$

$$t^- = \int \frac{ds}{C + \delta c - |u \cdot \cos \theta|} \quad (2)$$

where  $t^+$  is the propagation time from Station A to B,  $t^-$  indicates the propagation time from B to A,  $L$  is the propagation path,  $\theta$  is the angle between the flow velocity  $u$  direction and the acoustic propagation path.  $C$  is the average sound speed.  $\delta c \ll C$  is the sound speed change caused by water temperature. From the measured  $t^+$  and  $t^-$ , the sound speed can be estimated as:

$$C = \frac{L}{2} \left( \frac{1}{t^+} + \frac{1}{t^-} \right) \quad (3)$$

Then, for shallow water, the range-averaged temperature can be obtained based on the following formula [18]–[20]:

$$C_{S,T,P} = C_{0,0,0} + \Delta C_T + \Delta C_S + \Delta C_P + \Delta C_{STP} \quad (4)$$

where  $T$  and  $P$  represent temperature and pressure, respectively, and  $C_{0,0,0}$ ,  $\Delta C_T$ ,  $\Delta C_S$ ,  $\Delta C_P$ ,  $\Delta C_{STP}$  satisfy:

$$\begin{aligned} C_{0,0,0} &= 1402.392, \\ \Delta C_T &= 5.01109398873 \cdot T - 0.0550946843172 \cdot T^2 \\ &\quad + 0.000221535969240 \cdot T^3, \\ \Delta C_S &= 1.32952290781 \cdot S + 0.000128955756844 \cdot S^2, \\ \Delta C_P &= 0.15605925041 \cdot P + 0.0000244998688441 \cdot P^2 \\ &\quad - 0.88392332513 \cdot 10^{-8} \cdot P^3, \\ \Delta C_{STP} &= -0.0127562783426 \cdot T \cdot S \\ &\quad + 0.0063519163389 \cdot T \cdot P \\ &\quad + 0.265484716608 \cdot 10^{-7} \cdot T^2 \cdot P^2 \\ &\quad - 0.159349479045 \cdot 10^{-5} \cdot T \cdot P^2 \\ &\quad + 0.522116437235 \cdot 10^{-9} \cdot T \cdot P^3 \\ &\quad - 0.438031096213 \cdot 10^{-6} \cdot T^3 \cdot P \\ &\quad - 0.161674495909 \cdot 10^{-8} \cdot S^2 \cdot P^2 \\ &\quad + 0.968403156410 \cdot 10^{-4} \cdot T^2 \cdot S \\ &\quad + 0.485639620015 \cdot 10^{-5} \cdot T \cdot S^2 \cdot P \\ &\quad - 0.340597039004 \cdot T \cdot S \cdot P. \end{aligned}$$

Based on the above principle, a block diagram of HFAT is designed, as shown in Fig. 2, in which computer, data acquisition card, power amplifiers, filter amplifier, transmitting transducer, and hydrophone are given. In the transmitter, the

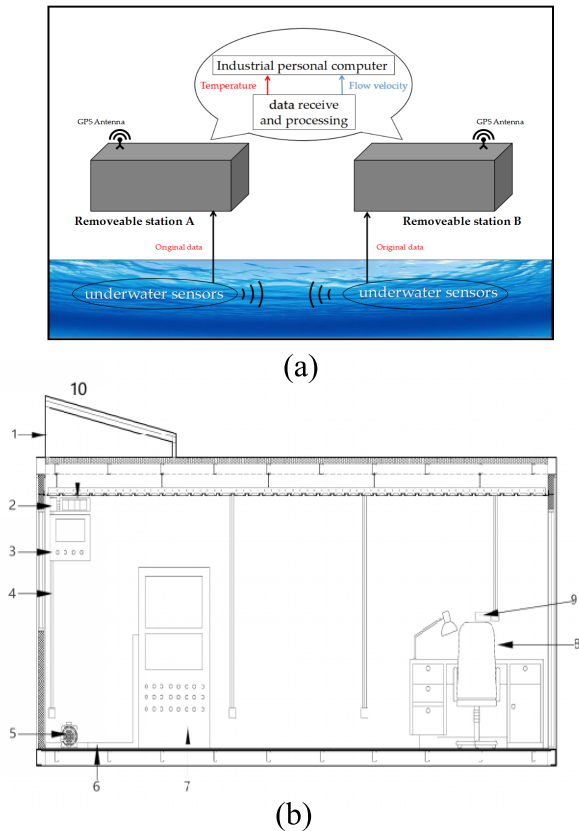


**FIGURE 1.** (a) Illustration of the HFAT system for real-time monitoring of range-averaged temperature in shallow water. For more details, see text. (b) Profile of the acoustic station including 1 solar panels, 2 external power interface, 3 emergency power supply, 4 power circuit, 5 water pump, 6 drain pipe, 7 real-time monitoring instrument, 8 work bench, 9 wireless Wifi, 10 power control.

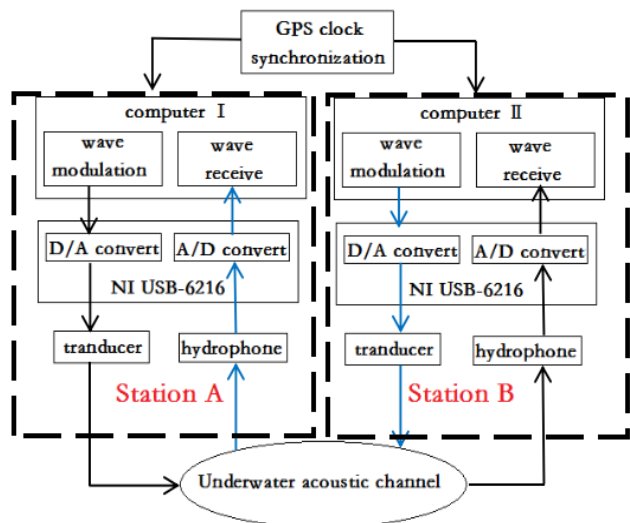


**FIGURE 2.** Systematic diagram of HFAT, where each acoustic station includes computer, data acquisition card, power amplifiers, filter amplifier, transmitting transducer, and hydrophone.

signal modulated by sine-wave 63-chip m sequence, is generated every 10-seconds by the computer. The electrical signal  $x(t)$  is then D/A converted by data acquisition card, power amplified, and transmitted by the acoustic transducer. In the receiver, acoustic signal is transformed into electrical signal by the hydrophone and filtered by an 8th-order Butterworth bandpass filter. After A/D conversion, the electric signal  $y(t)$  is sent into computer for further processing. The signal transmission and reception are synchronized with the GPS clock. The functions of all units of the HFAT system are given as:

1. GPS: Writes time message to computers and generates 1PPS (1 pulse per second) to trigger data acquisition card. The time precision of GPS is 20 ns.
2. Data acquisition card (NI USB-6216, National Instruments, USA): Performs A/D and D/A conversions with the sampling rate 400 kHz and receives 1PPS signals from GPS.
3. Power amplification: Increases the transmission power of underwater acoustic signals.
4. Filter amplification: Amplifies the received signal. An 8th-order Butterworth bandpass filter with the pass-band of 40-80 kHz is used to filter out the low frequency noise.
5. Acoustic transducer: As an acoustic transmitting sensor with central frequency of 60 kHz and bandwidth of 40 kHz, it transforms electrical signal  $x(t)$  into acoustic signal.
6. Hydrophone: As an acoustic receiving sensor with broad frequency range (from 1 kHz to 200 kHz) [22], it receives underwater acoustic signal and transforms acoustic signal into electrical signal  $y(t)$ .
7. In-situ thermometer: Water temperature sensor (In Situ Level TROLL 500, USA) is used to measure in-situ temperature for comparison. For Jiulong River,  $S$  and  $P$  of shallow fresh water were readily determined.

**III. EXPERIMENTAL RESULTS AND DISCUSSION**

We performed the HFAT experiment in the Jiulong River Estuary, as shown in Fig. 3. The Jiulong River Estuary is

a typical subtropical macro-tide estuary on the southwest coast of the Taiwan Strait. The study area in Zhangzhou City was from 117.783845° E-24.524548° N to 117.786112° E-24.521723° N. Acoustic transducers and hydrophones were deployed at two acoustic stations A and B with the distance of 390 m and the depth of 0.5m above the river floor.

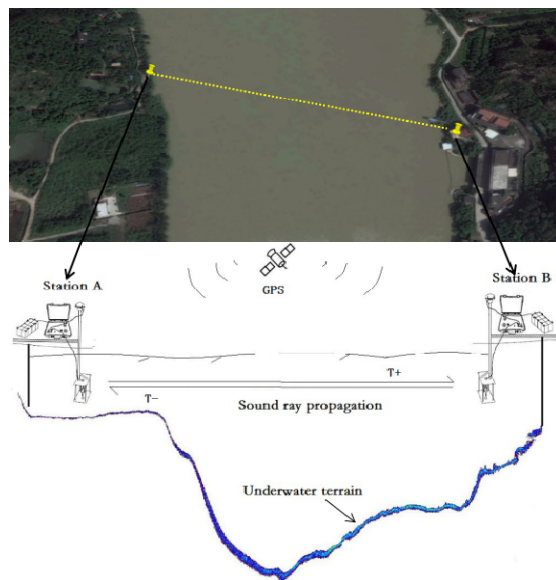


**FIGURE 3.** Map of the field experimental site and the acoustic reciprocal transmission of acoustic stations A and B.

From the cross-correlation analysis in Fig. 4, the propagation time  $t^+ = 0.263797$  s of the underwater acoustic wave from station A to B was estimated, while the propagation time  $t^- = 0.263805$  s from B to A was estimated. Higher  $t^-$  than  $t^+$  is associated with the current direction of Jiulong River from A to B. Based on  $t^+$  and  $t^-$ , the range averaged temperature was estimated as  $T = 23.95^\circ$ . In addition, for 60 kHz frequency, the acoustic wave period was 16.7 ms, which is much larger than the time precision 20 ns of GPS. Thus, high resolution GPS significantly reduced the measurement error of propagation time. Furthermore, the measurement accuracy of propagation time increases with frequency. For example, 6 kHz leads to the measurement accuracy of  $\pm 0.29^\circ\text{C}$ , while 60 kHz leads to the higher accuracy of  $\pm 0.002^\circ\text{C}$ . In comparison with previous low frequency underwater acoustic sensing schemes [7]–[12], significantly higher frequencies (central frequency is 60 kHz) were applied in this study. Lower central frequencies such as 40 Hz [10], 100-to 200-Hz [7], 400 Hz [11], 5 kHz [16], and 15 kHz [15] might lead to lower time accuracy of low frequency acoustic thermometries, which might limit their applications in estuaries with small spatial scales and shallow waters. HFAT might provide a more valuable method to extract the range averaged temperature of small scale waters in estuaries and coastal oceans.

Furthermore, Figs. 5(a) and (c) show the received underwater acoustic signals and the corresponding cross-correlation function at the station A from 19:00 pm to 2:00 am,

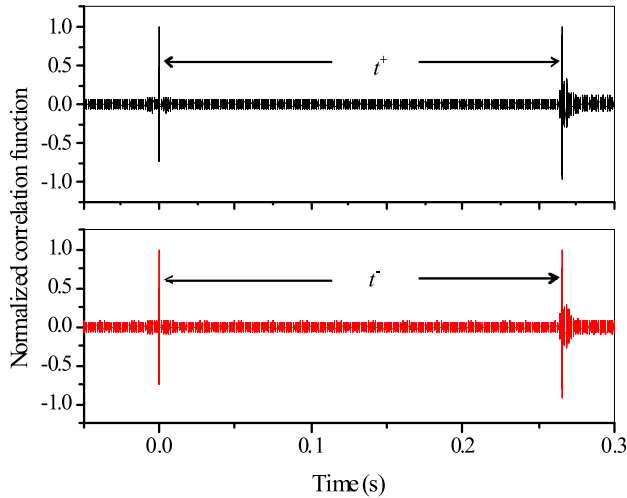


**FIGURE 4.** Acoustic propagation times  $t^+$  and  $t^-$  obtained by analyzing the cross-correlation function.

respectively, where the result at each hour was given. Figs. 5(b) and (d) give the selected waveform and the cross-correlation function at 22: 00 pm. During the experiments, the measured underwater signal waveforms were very stable. The signal-to-noise ratio was as high as 12 dB, indicating the efficiency of power amplification. The propagation times of underwater acoustic waves could be reliably estimated from the significantly high peaks in cross-correlation functions. These results demonstrate the effective performances of underwater acoustic sensors in HFAT. The measured acoustic signal has a certain tail, suggesting that the bandwidth of the underwater acoustic transducers could be further increased to improve the cross-correlation analysis. In addition, strong multi-path acoustic propagations were found in the river water. The first path corresponding to the first peak in the cross-correlation function might give the direct acoustic propagation. The second path corresponding to the second peak in the cross-correlation function mainly resulted from the propagation reflected by the water bottom. Due to larger propagation loss and bottom scattering [18], the signal amplitudes of the second path were lower than those of the first path.

In order to examine the reliability of HFAT, Fig. 6 compared in-situ temperatures measured by the temperature sensor with range-averaged temperatures measured by HFAT. Measurements were performed every thirty seconds. Two curves show the similar temperature change tendency because the weather cooled down in the experiments. Their relative standard deviation was less than 6%. Such a small difference might be associated with their different measurement conditions: temperature sensor measured in-situ temperature near the riverside, while HFAT measured the ranged-averaged temperature over the whole river.

In addition, we performed linear regressions to determine the relationship between range-averaged and

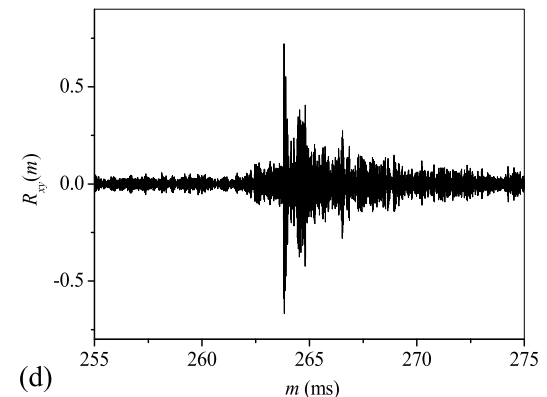
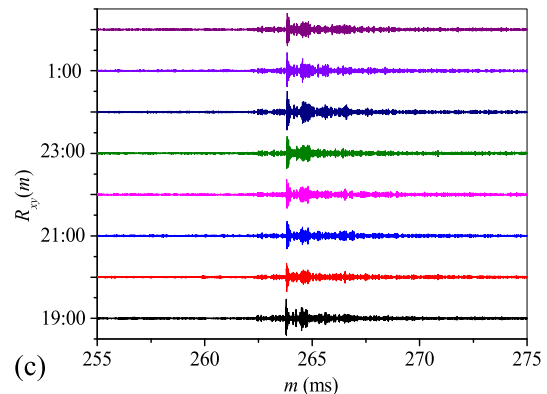
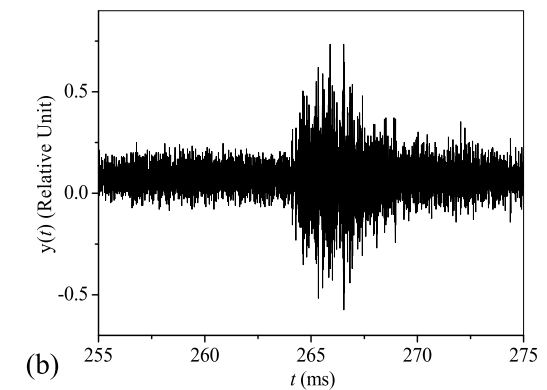
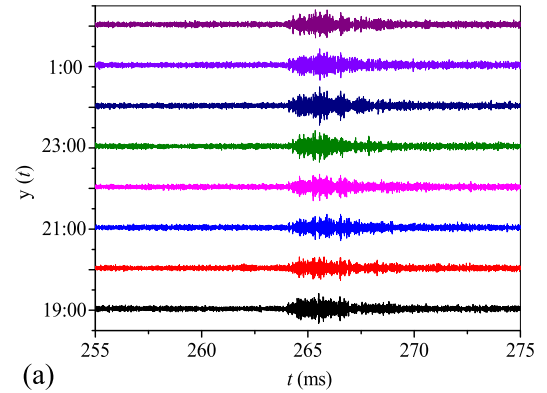


**FIGURE 5.** (a) The received underwater acoustic signals at the station A from 19: 00 pm to 2: 00 am, and (b) the selected signal at 22:00 pm. (c) The corresponding cross-correlation function results from 19: 00 pm to 2: 00 am, and (d) the selected result at 22:00 pm.



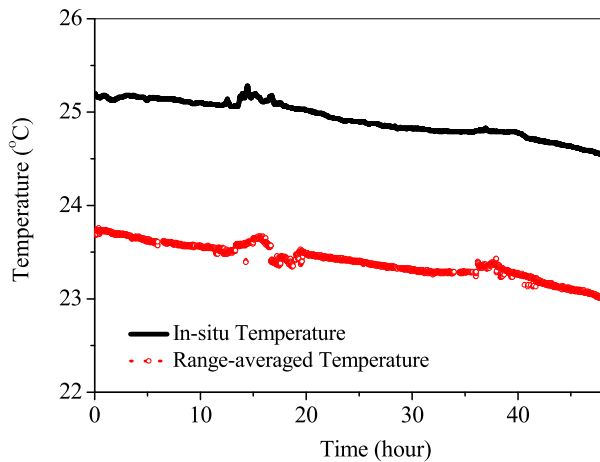


**FIGURE 6.** Comparison between range-averaged and in-situ temperatures, where the 48-hour experimental measurement was performed every thirty seconds.

in-situ temperatures. The linear correlation relationship was found as:

$$T(\text{average}) = 0.927T(\text{in-situ}) + 0.288, (R^2 = 0.98) \quad (5)$$

Clearly, the range-averaged temperatures matched the precision of those were measured with the in-situ temperature sensors. It should be noted that direct measurement of range-averaged temperature is difficult for in-situ sensors due to highly variant coastal ocean and estuarine waters [14]–[16]. As a result, in-situ temperature may not provide overall information of underwater environments. Tomography may play an important role to reconstruct the system parameter [7]–[11], [23]. HFAT, therefore, presents a valuable instrument for monitoring averaged temperature in shallow water areas, such as coastal oceans and estuaries. Eq. 5 gave a calibration formulism between range-averaged temperature and in-situ temperature. Combined with underwater acoustic sensor network [3]–[6], HFAT could be further developed for underwater environment monitoring network. Further studies should be performed in this important topic.

#### IV. CONCLUSION

In this paper, we proposed a new high frequency underwater acoustic scheme to measure range-averaged temperature in shallow waters. Reciprocal acoustic transmission, cross-correlation analysis, and GPS synchronization were used to derive the propagation times of underwater acoustic signals with the central frequency of 60 kHz, and thus measured the water temperature. The field experiment to evaluate the system accuracy was performed in the Jiulong River Estuary on the southwest coast of the Taiwan Strait. The underwater signal amplitudes were 12 dB higher than background noises. The range-averaged temperature by HFAT showed a good agreement with the in-situ temperature with a relative standard deviation of about 1.7%. During the experiment, range-averaged temperature was correlated with the in-situ temperature. The monitoring systems were built on Jiulong

riversides, differing from in-situ temperature sensors that were deployed in the middle of river. Such a setup might reduce the risk of being destroyed under extreme weather conditions in coastal and estuarine areas, such as heavy rain and flooding. The proposed HFAT scheme overcomes the limitations of existing in-situ temperature measuring methods. It might be valuable for monitoring real-time range-averaged underwater temperature in order to track the impacts of extreme weather and other climate events on coastal oceans and estuaries.

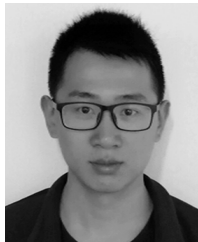
#### REFERENCES

- [1] K. M. Jeffrie et al., "Effects of high temperatures on threatened estuarine fishes during periods of extreme drought," *J. Exp. Biol.*, vol. 219, pp. 1705–1716, Mar. 2016.
- [2] M. A. Geawhari, L. Huff, N. Mhammdi, A. Trakadas, and A. Ammar, "Spatial-temporal distribution of salinity and temperature in the Oued Loukkos estuary, Morocco: Using vertical salinity gradient for estuary classification," *SpringerPlus*, vol. 3, p. 643, Oct. 2014.
- [3] G. Han, S. Shen, H. Song, T. Yang, and W. Zhang, "A stratification-based data collection scheme in underwater acoustic sensor networks," *IEEE Trans. Veh. Technol.*, vol. 67, no. 11, pp. 10671–10682, Nov. 2018.
- [4] G. Han, J. Jiang, L. Shu, and M. Guizani, "An attack-resistant trust model based on multidimensional trust metrics in underwater acoustic sensor network," *IEEE Trans. Mobile Comput.*, vol. 14, no. 12, pp. 2447–2459, Dec. 2015.
- [5] J. Jiang, G. Han, C. Zhu, S. Chan, and J. J. P. C. Rodrigues, "A trust cloud model for underwater wireless sensor networks," *IEEE Commun. Mag.*, vol. 55, no. 3, pp. 110–116, Mar. 2017.
- [6] J. Jiang, G. Han, L. Shu, S. Chan, and K. Wang, "A trust model based on cloud theory in underwater acoustic sensor networks," *IEEE Trans. Ind. Informat.*, vol. 13, no. 1, pp. 342–350, Feb. 2017.
- [7] W. Munk and C. Wunsch, "Ocean acoustic tomography: A scheme for large scale monitoring," *Deep Sea Res.*, vol. 26, pp. 123–161, Sep. 1979.
- [8] U. Send, F. Schott, F. Gaillard, and Y. Desaubies, "Observation of a deep convection regime with acoustic tomography," *J. Geophys. Res. Oceans*, vol. 100, no. C4, pp. 6927–6941, 1995.
- [9] B. D. Dushaw, "Inversion of multimegahertz-range acoustic data for ocean temperature," *IEEE J. Ocean. Eng.*, vol. 24, no. 2, pp. 215–223, Apr. 1999.
- [10] G. Duckworth, K. LePage, and T. Farrel, "Low-frequency long-range propagation and reverberation in the central Arctic: Analysis of experimental results," *J. Acoust. Soc. Amer.*, vol. 110, no. 1, pp. 747–760, 2001.
- [11] U. Send et al., "Acoustic observations of heat content across the Mediterranean Sea," *Nature*, vol. 385, pp. 615–617, Feb. 1997.
- [12] E. C. Shang, A. G. Voronovich, Y. Y. Wang, K. Naugolnykh, and L. Ostrovsky, "New schemes of ocean acoustic tomography," *J. Comput. Acoust.*, vol. 8, no. 3, pp. 459–471, 2000.
- [13] J.-H. Park and A. Kaneko, "Computer simulation of coastal acoustic tomography by a two-dimensional vortex model," *J. Oceanogr.*, vol. 57, no. 5, pp. 593–602, 2001.
- [14] A. Tolstoy, "Tomographic inversion for geoacoustic parameters in shallow water," *J. Comput. Acoust.*, vol. 8, no. 2, pp. 285–293, 2000.
- [15] Y. Zhang, Z. Zhao, D. Chen, and W. Yang, "High frequency ocean acoustic tomography observation at coastal estuary areas," *J. Acoust. Soc. Amer.*, vol. 131, no. 4, p. 3314, 2012.
- [16] X.-H. Zhu, C. Zhang, Q. Wu, A. Kaneko, X. Fan, and B. Li, "Measuring discharge in a river with tidal bores by use of the coastal acoustic tomography system," *Estuarine, Coastal Shelf Sci.*, vols. 104–105, pp. 54–65, Jun. 2012.
- [17] J. L. Spiesberger, "Ocean acoustic tomography: Travel time biases," *J. Acoust. Soc. Amer.*, vol. 77, no. 1, pp. 83–100, 1985.
- [18] R. J. Urick, *Principles of Underwater Sound*, 2nd Ed. New York, NY, USA: McGraw-Hill, 1975.
- [19] V. A. Del Grosso, "New equation for the speed of sound in natural waters (with comparisons to other equations)," *J. Acoust. Soc. Amer.*, vol. 56, no. 4, pp. 1084–1091, 1974.
- [20] P. F. Worcester, "Reciprocal acoustic transmission in a midocean environment," *J. Acoust. Soc. Amer.*, vol. 62, no. 4, p. 895, 1977.

- [21] X. Yu and Z. Zhang, "Ray chaos in an architectural acoustic semi-stadium system," *Chaos*, vol. 23, no. 1, 2013, Art. no. 013107.
- [22] Y. Zhang, Z. Song, X. Wang, C. Cao, and W. W. L. Au, "Directional acoustic wave manipulation by a porpoise via multiphase forehead structure," *Phys. Rev. Appl.*, vol. 8, Dec. 2017, Art. no. 064002.
- [23] M. Dai, X. Chen, M. Chen, H. Lin, F. Li, and S. Chen, "A novel method to detect interface of conductivity changes in magneto-acousto-electrical tomography using chirp signal excitation method," *IEEE Access*, vol. 6, pp. 33503–33512, 2018.



**XIAOJIAN YU** received the master's degree in landscape architecture from the University of Wisconsin–Madison, USA. She is currently an Associate Professor with the School of Biological Science and Biotechnology, Minnan Normal University. Her research interests include smart city sensing, urban planning and theory, architectural acoustics, 3-D model, and city spatial analysis based on complexity theory.



**XIAOBING ZHUANG** received the B.S. degree in marine physics from Xiamen University, Xiamen, China, in 2016. He is currently pursuing the M.S. degree with the College of Ocean and Earth Science, Xiamen University.

Since 2017, he was a Research Assistant with the Key Laboratory of Underwater Acoustic Communication and Marine Information Technology of the Ministry of Education. His research interest includes monitoring water velocity and temperature by using coastal acoustic tomography and underwater acoustic communication. He was a recipient of the Chinese Government Scholarship for his master's degree, in 2018.



**YANLONG LI** received the B.S. degree in engineering from the Henan University of Urban Construction, China, in 2015. He is currently pursuing the M.S. degree in architecture with Xiamen University. His research interests include architecture design, 3-D model, self-organization, and fractal in community.



**YU ZHANG** received the Ph.D. degree in acoustics from Nanjing University.

He has involved in scientific research at Northwestern University, University of Wisconsin–Madison, USA, and Xiamen University, China, in the fields of underwater acoustics, biosonar, and bionics. He is currently a Professor of underwater acoustic communication and marine information technology with Xiamen University. He has published 101 SCI papers in the field.

In 2012, he was selected as the second batch of high-level innovative talents and received the Science Fund for Distinguished Young Scholars of Fujian Province. He served as a Reviewer of the journals, including the *Physics Review Letters*, the *Journal of the Acoustical Society of America*, the *Electronics Letters*, and the *IEEE SIGNAL PROCESSING LETTERS*.

• • •